



## A single-column ocean-biogeochemistry model (GOTM-TOPAZ) version 1.0

Hyun-Chae Jung<sup>1</sup>, Byung-Kwon Moon<sup>1</sup>, Jieun Wie<sup>1</sup>, Hye-Sun Park<sup>2</sup>, Johan Lee<sup>3</sup>, Young-Hwa Byun<sup>3</sup>

<sup>1</sup>Division of Science Education, Institute of Fusion Science, Chonbuk National University, Jeonju 54896, South Korea

5 <sup>2</sup>Cray Korea Inc., Seoul 08511, South Korea

<sup>3</sup>National Institute of Meteorological Sciences, Seogwipo 63568, South Korea

*Correspondence to:* Byung-Kwon Moon ([moonbk@jbnu.ac.kr](mailto:moonbk@jbnu.ac.kr))

**Abstract.** Recently, Earth System Models (ESMs) have begun to consider the marine ecosystem to reduce errors in climate simulations. However, many models are unable to fully represent the ocean biology-induced climate feedback, which is due  
10 in part to a significant amount of bias in the simulated biogeochemical properties. We developed the Generic Ocean Turbulence Model–Tracers of Phytoplankton with Allometric Zooplankton (GOTM-TOPAZ) model, a single-column ocean-biogeochemistry model, which can be used to improve the ocean-biogeochemical processes of ESMs. This model was developed by combining GOTM, a single-column model (SCM) that can simulate the ocean’s physical environment, and TOPAZ, a biogeochemical module. Here, the original form of TOPAZ was modified and modularized to allow easy coupling  
15 with other ocean physical models. For interactions between the ocean physics and biogeochemical processes, the model was designed to allow the ocean temperature to change due to absorption of visible light by phytoplankton chlorophyll. We also added a module to reproduce upwelling and the air-sea gas transfer process for O<sub>2</sub> and CO<sub>2</sub>, which are of particular importance for marine ecosystems. To evaluate the simulation performance of GOTM-TOPAZ, simulated variables (e.g., chlorophyll, oxygen, nitrogen, phosphorus, silicon) were compared against observations. Our newly developed GOTM-  
20 TOPAZ model was able to capture the observed the temporal variations of upper-ocean chlorophyll reasonably well. Moreover, the simulated levels of dissolved oxygen, nitrogen, phosphorus, and silicon were consistent with the observations, which confirmed that GOTM-TOPAZ is reliable enough to be used in studies on climate systems. In particular, the TOPAZ module developed in this study may be used to couple complex biogeochemical processes with various ocean global circulation models and contribute to improved understanding of the feedback between climate and ocean-biogeochemical  
25 processes.

### 1 Introduction

For decades, climate researchers have accumulated a significant amount of knowledge on atmosphere-land-ocean feedback processes through various studies related to climate systems. With the advancement of coupled modeling techniques and the  
30 exponential increase in the number of computer resources available, climate research institutions worldwide began



competing to develop Earth System Models (ESMs). ESMs are often coupled with a biogeochemistry model that considers the atmosphere–ocean carbon cycle and ocean ecosystem cycle (Dunne et al. 2012b; Yool et al., 2013; Azhar et al., 2014; Stock et al., 2014; Aumont et al., 2015). Recently, the reproduction of ocean ecosystems with ESMs has become very precise with the addition of physiological details, such as light or nutrient acclimation, and the division of various phytoplankton and zooplankton into functional groups (Hense et al., 2017).

5  
10  
15  
20  
25  
Generally, the most important processes that are considered in ocean-biogeochemistry models are as follows: the ocean ecosystem cycle, including phytoplankton and zooplankton; the biogeochemical cycle of carbon; and the biogeochemical cycle of main nutrients (P, N, Fe, and Si) (Dunne et al., 2012b; Aumont et al., 2015). These three cycles are not independent and can participate in material exchange with each other through chemical mechanisms. There is still no consensus among researchers on methods for differentiating biogeochemical variables and methodologies for mathematization of biogeochemical processes; thus, they are mostly expressed via empirical relationships (Sauerland et al., 2018). In other words, biogeochemical processes are reproduced in the model through a parameterization that adjusts the parameters of the formula based on observations, and, in general, some parameters (e.g., maximum phytoplankton growth rate) are adjusted until the model produces reasonable results (Sauerland et al., 2018).

15  
20  
25  
Researchers have been using the single-column model (SCM) to control the parameterization method and to increase their understanding of the model physical processes. Betts and Miller (1986) suggested that the SCM is an effective tool for developing and controlling the convective scheme of an atmospheric model, while Price et al. (1986) used an ocean SCM for studying the daily cycle of the Pacific Ocean mixed layer. The SCM allows the physics parameterization to be controlled alongside large-scale forcing influences, and it has a low calculation cost, unlike 3D models. Accordingly, the SCM has been viewed as an essential tool for developing and improving numerical models (Lebassi-Habtezion and Caldwell, 2015; Hartung et al., 2018). In particular, because ocean-biogeochemical processes are reproduced inside the climate model based on column physics, the SCM-based studies are essential for improving ocean-biogeochemical processes (Evans and Garçon, 1997; Burchard et al., 2006; Bruggenman and Bolding, 2014). Even the latest analyses of the ESMs that participated in the fifth phase of the Coupled Model Intercomparison Project (CMIP5) show high bias and inter-model diversity for ocean-biogeochemical variables (Lim et al., 2017). Therefore, a single-column form of a biogeochemistry model should be an excellent tool for meeting the ongoing demand for improving the biogeochemistry model of the ESMs.

30  
The ocean biogeochemical cycle not only affects the physical environment of the upper ocean but that of the entire climate system as well, and such changes have feedbacks that, in turn, alter the ocean ecosystem (Hense et al., 2017; Lim et al., 2017; Park et al., 2018). Hense et al. (2017) presented the CO<sub>2</sub> cycle, gas and particle cycle, and changes in the physical environment of the upper ocean by chlorophyll as important climate-ocean biogeochemistry feedbacks reproduced in currently available ESMs. However, an ESM that reproduces all three of these biological mechanisms does not exist today. To reduce the uncertainty in predicting future climate change, all of these mechanisms need to be properly reproduced in the ESMs, which would allow them to evolve into a fundamentally different type of ESM. Generally, there are time constraints in repeated experiments using ocean global circulation models (OGCMs) and biogeochemistry models due to their



complexity and the large amount of calculation required. Consequently, the SCM is crucial for applying and testing new climate-ocean-biogeochemistry feedbacks in existing ESMs.

In this study, we developed the Generic Ocean Turbulence Model–Tracers of Phytoplankton with Allometric Zooplankton (GOTM-TOPAZ) model, which is a type of single-column ocean-biogeochemistry model. GOTM is a one-dimensional ocean model that focuses on reproducing the statistical turbulence closure (see <http://www.gotm.net>); TOPAZ is an ocean-biogeochemistry model developed by the Geophysical Fluid Dynamics Laboratory (GFDL), which is coupled with ESM2M and ESM2G (Dunne et al., 2012a; Dunne et al., 2012b). We modularized TOPAZ to apply the physical environment needed from the outside while also modifying it to be an SCM. This model was combined with GOTM, to which an air-sea gas exchange for CO<sub>2</sub> and O<sub>2</sub> and optical feedback from photosynthesis by chlorophyll were implemented. In addition, a w-  
 5 advection prescription module that can reproduce upwelling was also added. To verify the model, we selected points in the East/Japan Sea off the coast of the Korean Peninsula and conducted simulations. The results produced by GOTM-TOPAZ were compared to observed data and results from OGCMs to verify the reliability of the model.

## 2 Ocean Physical Model: General Ocean Turbulence Model (GOTM)

15 In GOTM-TOPAZ, GOTM version 4.0 is responsible for the ocean physics. The physical basis of GOTM lies with the Reynolds-averaged Navier–Stokes equations in a rotational coordinate system (Eqs. 1 and 2). Moreover, the temperature and salinity equations derived by such a method are represented by Eqs. 3 and 4, respectively. GOTM calculates a one-dimensional version of potential temperature, salinity, and horizontal velocity based on these four equations:

$$20 \quad \partial_t u - \nu \partial_{zz} u + \partial_z \langle u'w' \rangle = -\frac{1}{\rho_0} \partial_x p + fv, \quad (1)$$

$$\partial_t v - \nu \partial_{zz} v + \partial_z \langle v'w' \rangle = -\frac{1}{\rho_0} \partial_y p - fu, \quad (2)$$

$$\partial_t T - \dot{\nu} \partial_{zz} T + \partial_z \langle w'T' \rangle = \frac{\partial_z I}{c_p \rho_0}, \quad (3)$$

$$\partial_t S - \dot{\nu} \partial_{zz} S + \partial_z \langle w'S' \rangle = \tau_R^{-1} (S_R - S). \quad (4)$$

25 In Eqs. (1) and (2),  $\nu$  represents the molecular diffusivity of momentum;  $\rho_0$  is a constant reference density;  $p$  is pressure; and  $f$  represents the Coriolis parameter. In the temperature equation, Eq. (3),  $\dot{\nu}$  represents the molecular diffusivity due to heat;  $c_p$  represents the heat capacity; and  $I$  represents the vertical divergence of short-wave radiation. In the temperature equation, the effect of solar radiation absorbed by seawater is included, and, thus, Eq. (3) is closely associated with the radiation parameterization method. Moreover, an ocean-biogeochemistry coupled model must contain an additional short-  
 30 wave absorption process associated with chlorophyll synthesis distributed throughout the upper-ocean layer (Morel and



Antoine, 1994; Cloern et al., 1995; Manizza et al., 2005; Litchman et al., 2015; Hense et al., 2017). Based on the methodology by Manizza et al. (2005), we applied a visible light absorption process due to chlorophyll synthesis to the coupled model, which will be explained in detail in Section 4.5. Equation (4) is an equation that explains the vertical distribution of salinity. In this equation,  $\nu''$  represents the molecular diffusivity of salinity;  $\tau_R$  represents the relaxation time scale; and  $S_R$  represents the observed salinity distribution. In other words, the terms on the right side of the salinity equation express the “relaxation” process based on observations. Unlike 3D models, SCMs cannot reproduce horizontal advection. Therefore, for salinity, which is greatly affected by horizontal advection, it is necessary to prescribe and supplement the observed value to the simulated value, as with the terms on the right side of Eq. (4) (Burchard et al., 2006). Please refer to Umlauf and Burchard (2003), Umlauf et al. (2005), Umlauf and Burchard (2005), and Burchard et al. (2006) for detailed information related to the GOTM.

### 3 Biogeochemistry Model: Tracers of Phytoplankton with Allometric Zooplankton (TOPAZ)

We used the TOPAZ2 version for coupling. TOPAZ simulates not only the ocean carbon cycle, but also nitrogen, phosphorus, iron, dissolved oxygen, and lithogenic material cycles, while also considering the growth cycles of zooplankton and phytoplankton. It divides phytoplankton into small and large groups based on size while also simulating the group of diazotrophs, which are nitrogen fixers. Consequently, TOPAZ handles a total of 30 types of prognostic tracers and 11 types of diagnostic tracers. The local changes in the tracers simulated in TOPAZ can be explained by the following equation:

$$\partial_t C = -\nabla \cdot \vec{v} C + \nabla K \nabla C + S_C. \quad (5)$$

Equation (5) is an advection-diffusion equation for each state variable  $C$  simulated in TOPAZ. In this equation,  $\vec{v}$  represents the velocity vector calculated in the ocean model, and  $K$  represents the diffusivity.  $S_C$  represents the sources minus sinks of state variable  $C$  calculated at each point in the model. TOPAZ receives input from the ocean model with respect to the transport tendency of tracers associated with advection and horizontal diffusion, while, for vertical diffusion, the sources minus sinks are calculated internally by TOPAZ. The biological processes of TOPAZ were reproduced with a focus on the growth of phytoplankton, nutrient limitation, light limitation, and the grazing process, and the empirical formulas derived from observations were used to establish the ocean ecosystem model (Dunne et al., 2012b). Please refer to Dunne et al. (2012b) for detailed information related to TOPAZ.



#### 4 Ocean-Biogeochemistry Coupled Model: GOTM-TOPAZ

TOPAZ is coupled with the Modular Ocean Model version 5 (MOM5), an OGCM developed by GFDL. We separated TOPAZ from MOM5 and constructed two modules by separating the initialization subroutine and main calculation subroutine. In addition, this model was modified into an SCM form while adding interfaces associated with the surface flux  
5 prescription (boundary condition) and initial data input.

In the coupled model, GOTM relayed the ocean physics to TOPAZ, whereby TOPAZ relayed the optical feedback of chlorophyll simulated according to the ocean physics to GOTM. A subroutine that calculates the optical feedback from chlorophyll and another subroutine for the prescription of w-advection were added to GOTM-TOPAZ (See Fig. 1 for the flow diagram). Upwelling that usually occurs along the coastal area due to wind plays a major role in changing the vertical  
10 distribution of zooplankton and phytoplankton by supplying the surface layer with nutrient-rich intermediate water (Krezel et al., 2005; Lips and Lips, 2010; Shin et al., 2017). We used the module related to w-advection in GOTM to allow upwelling to be reproduced in TOPAZ.

##### 4.1 Initial Conditions

15 The initial data needed to operate GOTM-TOPAZ can be divided into data needed to operate the GOTM and TOPAZ models individually. First, to operate GOTM, water temperature and salinity data at the initial time and salinity data while in operation were determined. The salinity data while in operation are needed for the relaxation of GOTM. With respect to TOPAZ, the initial data for prognostic (30 types) and diagnostic (11 types) tracers are needed.

##### 20 4.2 Boundary Conditions

Because GOTM-TOPAZ is not coupled with an atmosphere model, atmospheric forcing data must be prescribed. The atmospheric forcing variables needed to operate the model are as follows: 10 m u-wind, v-wind [ $\text{m s}^{-1}$ ], surface (2 m) air pressure [hPa], surface (2 m) air temperature [ $^{\circ}\text{C}$ ], relative humidity [%] or wet bulb temperature [ $^{\circ}\text{C}$ ] or dew point temperature [ $^{\circ}\text{C}$ ], and cloud cover [1/10].

25 To accurately simulate ocean-biogeochemical variables, surface or bottom flux values for a few types of tracers must be given. TOPAZ possesses a process for calculating the bottom flux generated by sediment within the module (Dunne et al., 2012b). However, TOPAZ does not possess a process for calculating the flux value provided from the atmosphere to the ocean surface. Therefore, we added processes for calculating the surface flux of  $\text{O}_2$ ,  $\text{NO}_3$ ,  $\text{NH}_4$ , alkalinity, lithogenic aluminosilicate, dissolved iron, and dissolved inorganic carbon. The surface flux calculation process is implemented within  
30 `generic_topaz_column_physics` among the subroutines shown in Fig. 1. The surface flux of  $\text{NO}_3$ ,  $\text{NH}_4$ , lithogenic aluminosilicate, and dissolved iron is prescribed by monthly average climate values, while alkalinity is calculated by the



prescribed  $\text{NO}_3$  dry/wet deposition values. The following equation was used for the  $\text{O}_2$  and  $\text{CO}_2$  (dissolved inorganic carbon) air-sea gas transfer:

$$F = k_w \rho ([A] - [A]_{\text{sat}}). \quad (6)$$

5

Here,  $F$  is the upward flux of gas  $A$ , and  $k_w$  is the gas transfer velocity with respect to gas  $A$ . The gas transfer velocity can be calculated as a function of the Schmidt number and wind speed at 10 m (Wanninkhof, 1992). In addition,  $[A]$  is the concentration of gas  $A$  at the ocean surface, while  $[A]_{\text{sat}}$  is the corresponding saturation concentration of gas  $A$  in equilibrium with a water-vapor-saturated atmosphere at total atmospheric pressure. Please refer to Najjar and Orr (1998) for detailed information related to Eq. (6).

10

### 4.3 Ocean Physics

GOTM simulates ocean physics environments based on Eqs. (1)–(4). In the coupled model, GOTM relays the simulated one-dimensional ocean physical variables to the TOPAZ module at each time step. The relayed variables are as follows: potential temperature [ $^{\circ}\text{C}$ ], salinity [psu], thermal diffusion coefficient [ $\text{m}^2 \text{sec}^{-1}$ ], density [ $\text{kg m}^{-3}$ ], thickness [m], mixed layer thickness [m], and radiation [ $\text{w m}^{-2}$ ].

15

### 4.4 Optical Feedback

As explained in Section 2, chlorophyll distributed throughout the upper ocean is known to have chemical and physical effects through its photosynthesis action. Manizza et al. (2005) used satellite observation data and OGCMs in conducting a study on changes in ocean irradiance due to the absorption of visible light by chlorophyll. We used the methodology by Manizza et al. (2005) and applied the optical feedback from chlorophyll on GOTM-TOPAZ in the following manner:

20

$$k_{\lambda} = k_{\text{sw}(\lambda)} + \chi_{(\lambda)} \cdot [\text{chl}]^{e(\lambda)}, \quad (7)$$

$$I_{\text{IR}} = I_0 \cdot 0.58, \quad (8)$$

$$I_{\text{VIS}} = I_0 \cdot 0.42, \quad (9)$$

$$I_{\text{RED}} = I_{\text{BLUE}} = \frac{I_{\text{VIS}}}{2}, \quad (10)$$

$$I_{(z)} = I_{\text{IR}} \cdot e^{-k_{\text{IR}z}} + I_{\text{RED}(z-1)} \cdot e^{-k_{(r)}\Delta z} + I_{\text{BLUE}(z-1)} \cdot e^{-k_{(b)}\Delta z}. \quad (11)$$

In this equation, visible light was divided into red and blue/green bands, in accordance with the method used by Manizza et al. (2005). In Eq. (7),  $\lambda$  represents the wavelength of the red or blue/green bands. Here,  $k_{\text{sw}(\lambda)}$  represents the light

30



attenuation coefficient of optically pure seawater, which has a value of  $0.225 \text{ m}^{-1}$  and  $0.0232 \text{ m}^{-1}$  for red and blue/green bands, respectively. For red and blue/green bands,  $\chi_{(\lambda)}$  has a value of 0.037 and  $0.074 \text{ m}^{-2} \text{ mg Chl m}^{-3}$ , respectively, and  $e_{(\lambda)}$  has a value of 0.629 and 0.674 [no units], respectively. Moreover, [chl] represents the concentration of chlorophyll with units of  $\text{mg Chl m}^{-3}$ .

5 Infrared light  $I_{IR}$  and visible light  $I_{VIS}$  that reach the mean open ocean conditions are set to Eqs. (8) and (9), respectively, by default. However, GOTM-TOPAZ can change the light extinction method by modifying the namelist of GOTM (see <http://www.gotm.net>), by which the coefficients of  $I_{IR}$  and  $I_{VIS}$  can also be changed. The total irradiance of the red and blue/green bands that reach the ocean surface is represented by Eq. (10). Ultimately, the irradiance of visible light transmitted for each vertical level ( $z$ ) can be calculated in GOTM-TOPAZ by Eq. (11). Moreover, the sum of the second and  
10 third terms on the right side of Eq. (11) represents photosynthetically active radiation (PAR), where PAR is used in TOPAZ to calculate the growth rate of phytoplankton groups.

#### 4.5 w-advection

As mentioned earlier, the upwelling phenomenon generated by coastal winds is known to affect plankton growth by  
15 supplying nutrient-rich intermediate water to the upper ocean. GOTM is already designed to allow the user to anthropogenically prescribe w-advection to experimental cases. We linked the subroutines of GOTM that are related to w-advection to TOPAZ so that the user can study the impact of upwelling on the biogeochemical environment. The user of the model can prescribe vertical advection as a constant or input the velocities by time and depth in ASCII format to reproduce the desired form of vertical motions. Please refer to GOTM's homepage (<http://www.gotm.net>) and Burchard et al. (2006)  
20 for technical details and numerical analysis related to w-advection prescription in GOTM.

## 5 Results

To verify GOTM-TOPAZ, we selected a point in the East/Japan Sea to construct a test case. The East/Japan Sea is unique with steep topography and three ocean basins that are semi-enclosed, large, and deep. Moreover, it is somewhat isolated  
25 from major oceans, connecting to the Pacific Ocean through a narrow strait, and is sometimes referred to as a miniature ocean since a double gyre is present and it experiences various oceanic phenomena (Ichiye, 1984). The high-temperature, high-salinity Tsushima Warm Current (TWC) introduced through the Korea Strait is divided into two main branches: the Nearshore Branch (NB) that flows northeastward along the Japanese coast and the East Korea Warm Current (EKWC) that flows northward along the Korean coast (Uda, 1934; Tanioka, 1968; Moriyasu, 1972). Between these two main branches,  
30 another branch exists offshore of the first branch (the Offshore Branch, OB), but it is not present all year (Shimomura and Miyata, 1957; Kawabe, 1982). In the north, the North Korea Cold Current (NKCC) flows southward along the coast of



Korea. The East/Japan Sea is divided into warm and cold regions relative to the 40° north latitude, and, since the current pattern and characteristics in the East/Japan Sea vary spatially and seasonally, they are very important to oceanographic studies. The southern coast of the Korean Peninsula has nutrient-rich seawater due to inflow from the Nakdong River, which is located on the southeast end of the Korean peninsula. Moreover, because of the influence of a strong southerly wind during the summer, upwelling occurs off the coast of the East/Japan Sea, and, as a result, seawater in this region has high concentrations of nutrients and phytoplankton. This seawater with high nutrient and chlorophyll levels is transported north of Ulleungdo by the EKWC. Due to these characteristics, the East/Japan Sea is considered an important biogeochemical research region (Joo et al., 2014; Kim et al., 2016; Shin et al., 2017). Thus, we selected a point in the East/Japan Sea (130.0°E, 38.0°N) where the EKWC and NKCC meet (Fig. 2).

In this study, we used the ocean observation data provided by the Korea Oceanographic Data Center of the National Institute of Fisheries Science (NIFS; <http://www.nifs.go.kr/kodc>) for seawater temperature data, initial salinity data, and salinity data during implementation for relaxation. Moreover, for the initial data on prognostic/diagnostic tracers of TOPAZ, we used the data provided for basic operation of MOM5. For atmospheric forcing data, we input 0.75° ERA-Interim reanalysis data provided by the ECMWF (Dee et al., 2011). We applied global data to the model through interpolation using the latitude and longitude values of the test scenario for calculations.

For the observational data on seawater temperature and salinity for verifying the results from GOTM-TOPAZ, we used the monthly average of the analysis fields in the EN.4.2.1 data provided by the Met Office Hadley Centre (Good et al., 2013) that were adjusted using the method by Gouretski and Reseghetti (2010). With respect to chlorophyll, Sea-viewing Wide Field-of-view Sensor (SeaWiFS) satellite observation data with a resolution of 9 km from October 1997 to December 2007, as provided by the NASA Goddard Space Flight Center (McClain et al., 1998), were compared with the results simulated by the model. The simulation results of nutrients, such as dissolved oxygen, nitrogen, phosphorus, and silicon, were tested using the aforementioned observational data from NIFS. Moreover, the data from the model that operated MOM4, the Sea-Ice Simulator, and TOPAZ together (MOM) were used for comparative analysis. MOM was operated by inputting Coordinated Ocean-ice Reference Experiments (CORE-II) forcing data (Large and Yeager, 2009) from 1950 to 2008.

25

### 5.1 East/Japan Sea Scenario (130.0°E/38.0°N)

We used observational data from the East/Japan Sea point to operate GOTM-TOPAZ from 1995 to 2008; four years (1995 to 1998) were defined as a spin-up period, and we then analyzed the results from 1999 to 2008. Figure 3 shows vertical sections over time of the MOM and GOTM-TOPAZ results and observational data (EN.4.2.1). As shown in Fig. 3, vertical spatial distributions of water temperature and salinity simulated by GOTM-TOPAZ were similar to the observational data. Of course, simulation of salinity by GOTM-TOPAZ can be similar to observational results since relaxation was applied. Generally, East Sea Intermediate Water (ESIW) with depths of 200–400 m is known for its high dissolved oxygen

30



concentration and the appearance of a salinity minimum layer (Kim and Chung, 1984; Kim and Kim, 1999). In Fig. 3, observational and MOM results showed that the water temperature was affected by ESIW, a finding that did not appear in the GOTM-TOPAZ results. It was determined that, since GOTM-TOPAZ could not reproduce ESIW advection, there were differences in the vertical distribution of water temperature and chlorophyll near water depths of 200 m when compared to  
5 the observational results. Despite this, the variables simulated by GOTM-TOPAZ showed seasonal variations that were similar to the observational and OGCM results (Fig. 3c).

In order to verify the results of the chlorophyll simulated by GOTM-TOPAZ, we used the SeaWiFS data. SeaWiFS measures the chlorophyll concentration by using the light reflected from the ocean surface. However, part of the reflected light reaches the satellite from the mixed layer below the ocean surface due to a backscattering effect (Jochum et al., 2009;  
10 Park et al., 2013). Therefore, we compared chlorophyll anomalies averaged up to 20 m of water depth in the data from each model and chlorophyll from SeaWiFS. Simulated chlorophyll distributed on the ocean surface (0–20 m) showed seasonal variations that were similar to the observational results (Fig. 4a). Compared to the observational results, the correlation coefficients of GOTM-TOPAZ and MOM were found to be 0.51 and 0.60, respectively. With respect to the maximum concentration of chlorophyll occurring annually on the surface layer, GOTM-TOPAZ showed smaller errors against the  
15 observational results than did MOM.

Chlorophyll at the East/Japan Sea point is distributed mostly around water depths of 40 m (Fig. 3). Accordingly, we averaged chlorophyll concentrations from 20 m to 80 m to verify the model results (Fig. 4b). However, since observational data for chlorophyll in the subsurface layer (~20–80 m) were unavailable, the MOM and GOTM-TOPAZ results were compared. Chlorophyll in the subsurface layer also showed slight differences in the scale of minimum and maximum values,  
20 but both models showed similar seasonal variations (Fig. 4b). However, when compared to the MOM results, the time series of the chlorophyll anomaly in the ocean surface and subsurface layers simulated by GOTM-TOPAZ appear to have a time shift (Fig. 4a,b). In the TOPAZ module of MOM, the transport tendencies of each tracer were calculated in the ocean model, but the same process was not carried out in GOTM-TOPAZ. Since the transport tendency is mainly determined by the horizontal advection, the difference in chlorophyll concentrations between the two models can be attributed mostly to  
25 horizontal advection. As mentioned in Section 5, a current with high nutrient and chlorophyll content is introduced into the northern region of Ulleungdo through the EKWC, mostly during the summer, which may also explain these chlorophyll anomaly time series differences.

We evaluated the simulation performance of GOTM-TOPAZ for dissolved oxygen, nitrogen, phosphorus, and silicon. Dissolved oxygen in the ocean surface simulated by GOTM-TOPAZ showed a seasonal variation that was similar to the  
30 observational and MOM results (Fig. 5a). These results can be viewed as validating the gas flux equation reproduced in GOTM-TOPAZ. The nutrient concentration on the ocean surface simulated by GOTM-TOPAZ showed a lower correlation with the observed data than did MOM, but the GOTM-TOPAZ results showed seasonal variations similar to those from MOM and the observations (Fig. 5b–d).



Figure 6 shows a comparison of vertical profiles of dissolved oxygen, nitrogen, phosphorus, and silicon averaged for February, August, and the entire period from 1999 to 2008. Mixing in the upper ocean occurs actively during winter due to strong winds. GOTM-TOPAZ accurately simulated dissolved oxygen and nutrient concentrations in the upper layer during the winter (Fig. 6a). At the East/Japan Sea point, the highest concentration of phytoplankton, which consume nutrients for growth, is found around depths of 40 m during the summer (Fig. 3). As a result, concentrations of nutrients such as nitrogen, phosphorus, and silicon in the upper layer decreased during August, and these concentrations are clearly distinguishable in each layer due to strong stratification during the summer (Fig. 6b). A similar pattern appeared in the observational and GOTM-TOPAZ results. Moreover, GOTM-TOPAZ properly simulated the increasing trend of dissolved oxygen due to photosynthesis at water depths (upper 80 m) where phytoplankton is highly concentrated (Fig. 6b). However, a highly concentrated dissolved oxygen concentration is not apparent in the observational data. Generally, the dissolved oxygen concentration in seawater transported by the EKWC is low, while the dissolved oxygen concentration at the East/Japan Sea point is relatively higher (Rho et al., 2012). It is possible that the high-concentration layer of the dissolved oxygen at the subsurface layer did not appear since the value was derived by averaging observational data over 10 years. Moreover, the concentrations from the surface to 250 m were very similar between GOTM-TOPAZ and the observational results. However, the difference in oxygen concentrations between the observational and model results increased beyond water depths of 250 m. We interpreted that the reason for such a difference in oxygen concentrations was due to GOTM-TOPAZ not being able to reproduce the ESIW. Nonetheless, the results demonstrated that, overall, GOTM-TOPAZ demonstrated an excellent simulation of dissolved oxygen and nutrients, all within range of the standard deviation of the observed values (Fig. 6c).

## 20 6 Discussion

In this paper, we have explained the major models that comprise GOTM-TOPAZ and the ocean-biogeochemical processes reproduced within the models. In addition, we compiled data from an East/Japan Sea point near the Korean Peninsula with oceanographic importance and analyzed the results of operating the model for a decade (~1999–2008). We compared ocean water temperatures, salinity, and biogeochemical variables, such as chlorophyll, dissolved oxygen, and nitrogen, against the observational data and OGCM output to evaluate the performance of GOTM-TOPAZ. The simulated vertical distributions and seasonal variations are found to be consistent with the observational data and OGCM output.

Although GOTM-TOPAZ exhibits a deficiency in reproducing the observations under the influence of enhanced currents, which is common for SCMs, it has the advantage of being able to easily simulate various sensitivity experiments (e.g., analyses on the effects of atmospheric forcing changes or chemical deposition on the physical and biogeochemical ocean environment). Therefore, GOTM-TOPAZ can be an excellent tool for researchers who study Earth systems while also contributing to parameterization improvements in ocean-biogeochemistry models and the consideration of various oceanic-biological mechanisms.



Of course, there are many issues in GOTM-TOPAZ that require improvement for its use in various fields of climate research. Sonntag and Hense (2011) used a simple biogeochemistry model linked to GOTM (GOTM-BIO) to analyze the effects of phytoplankton on the physical environment of the upper ocean. In particular, the feedback from cyanobacteria during surface blooms that cause changes in ocean surface albedo, solar light absorption rate, and amount of momentum relayed to the ocean by wind were applied to the model in conducting the experiment. This study allowed us to better understand the development needs and direction for GOTM-TOPAZ, and we plan to apply various climate-ocean biogeochemistry feedback mechanisms in future research. In addition, we also plan to evolve GOTM-TOPAZ into a single ES

5

10 We separated TOPAZ from its coupling with MOM and constructed the model with a separate initiation module and column physics module, which introduced the possibility of coupling it with various ocean models in the future more easily. Currently, we are conducting a study on coupling TOPAZ with the Nucleus for European Modelling of the Ocean (NEMO), another type of OGCM. NEMO is already coupled with other biogeochemistry models, such as the Model of Ecosystem Dynamics, Nutrient Utilization, Sequestration and Acidification (MEDUSA, Yool et al., 2013), and the Pelagic Interactions

15 Scheme for Carbon and Ecosystem Studies (PISCES, Aumont et al., 2015). If NEMO and TOPAZ can be coupled successfully, a comparative analysis can be conducted on the simulation results from the three models, which may provide the driving force for improving the physical processes associated with ocean-biogeochemistry.

**Code and data availability:**

20 The GOTM-TOPAZ software is based on GOTM version 4 and MOM version 5, both available for download from their respective distribution sites (<https://gotm.net>, <https://www.gfdl.noaa.gov/>), and it is freely available at <https://doi.org/10.5281/zenodo.1405270>.

**Author contribution:**

25 H.C.J. and B.K.M. drafted the paper, performed the experiments, and were primarily responsible for developing GOTM-TOPAZ. J.W., H.S.P., J.L., and Y.H.B. contributed to code debugging and the writing of this paper.



**Competing interests:**

The authors declare that they have no conflict of interest.

**Acknowledgements:**

5 We would like to thank the GOTM and MOM communities for their support. In addition, we would like thank ECMWF for providing ERA-Interim data and Met Office Hadley Centre for providing EN4 datasets. In addition, we would like to thank NIFS for providing ocean observation data. We would also like to thank NASA Goddard Space Flight Center for providing SeaWiFS datasets. We also thank D.H Kim at Kongju University of Korea for providing some advice during this research. This work was funded by the Korea Meteorological Administration Research and Development Program under Grant  
10 KMI(KMI2018-03513).



## References

- Aumont, O., Ethe, C., Tagliabue, A., Bopp, L., and Gehlen, M.: PISCES-v2: an ocean biogeochemical model for carbon and ecosystem studies, *Geosci. Model Dev.*, 8, 2465–2513, doi:10.5194/gmd-8-2465-2015, 2015.
- Azhar, M. A., Canfield, D. E., Fennel, K., Thamdrup, B., and Bjerrum, C. J.: A model-based insight into the coupling of nitrogen and sulphur cycles in a coastal upwelling system, *J. Geophys. Res. Biogeosci.*, 119, 264–285, doi:10.1002/2012JG002271, 2014.
- 5 Betts, A. K., and Miller, M. J.: A new convective adjustment scheme. Part II: Single column tests using GATE wave, BOMEX, ATEX and arctic air-mass data sets, *Q. J. Roy. Meteor. Soc.*, 112, 693–709, doi:10.1002/qj.49711247308, 1986.
- 10 Bruggeman, J., and Bolding, K.: A general framework for aquatic biogeochemical models, *Environ. Modell. Softw.*, 61, 249–265, doi:10.1016/j.envsoft.2014.04.002, 2014.
- Burchard, H., Bolding, K., Kuhn, W., Meister, A., Neumann, T., and Umlauf, L.: Description of a flexible and extendable physical-biogeochemical model system for the water column, *J. Marine Syst.*, 61, 180–211, doi:10.1016/j.jmarsys.2005.04.011, 2006.
- 15 Cloern, J. E., Grenz, C., and Videgar-Lucas, L.: An empirical model of the phytoplankton chlorophyll: carbon ratio—the conversion factor between productivity and growth rate, *Limnol. Oceanogr.*, 40(7), 1313–1321, doi:10.4319/lo.1995.40.7.1313, 1995.
- Dee, D. P., Uppala, S. M., Simmons, A. J., Berrisford, P., Poli, P., Kobayashi, S., Andrae, U., Balmaseda, M. A., Balsamo, G., Bauer, P., Bechtold, P., Beljaars, A. C. M., van de Berg, L., Bidlot, J., Bormann, N., Delsol, C., Dragani, R., Fuentes, M., Geer, A. J., Haimberger, L., Healy, S. B., Hersbach, H., Hólm, E. V., Isaksen, I., Kållberg, P., Köhler, M., Matricardi, M., McNally, A. P., Monge-Sanz, B. M., Morcrette, J.-J., Park, B.-K., Peubey, C., de Rosnay, P., Tavolato, C., Thépaut, J.-N., and Vitart, F.: The ERA-Interim reanalysis: configuration and performance of the data assimilation system, *Q. J. R. Meteorol. Soc.*, 137, 553–597, doi:10.1002/qj.828, 2011.
- 20 Dunne, J. P., John, J. G., Adcroft, A. J., Griffies, S. M., Hallberg, R. W., Shevliakova, E. N., Stouffer, R. J., Cooke, W., Dunne, K. A., Harrison, M. J., Krasting, J. P., Malyshev, S. L., Milly, P. C. D., Philipps, P. J., Sentman, L. A., Samuels, B. L., Spelman, M. J., Winton, M., Wittenberg, A. T., and Zadeh, N.: GFDL’s ESM2 global coupled climate-carbon Earth System Models Part I: Physical formulation and baseline simulation characteristics, *J. Clim.*, doi:10.1175/JCLI-D-11-00560.1, 2012a.
- 30 Dunne, J. P., John, J. G., Shevliakova, E., Stouffer, R. J., Krasting, J. P., Malyshev, S. L., Milly, P. C. D., Sentman, L. T., Adcroft, A. J., Cooke, W., Dunne, K. A., Griffies, S. M., Hallberg, R. W., Harrison, M. J., Levy, H., Wittenberg, A. T., Philipps, P. J., and Zadeh, N.: GFDL’s ESM2 global coupled climate-carbon earth system models. Part II: carbon system formulation and baseline simulation characteristics, *J. Clim.*, 26, 2247–2267, doi:10.1175/jcli-d-12-00150.1, 2012b.



- Evans, T., and Garçon, V.: One-Dimensional Models of Water Column Biogeochemistry; Report of a Workshop held in Toulouse, France; November-December 1995, Editors, February, 1997.
- Good, S. A., Martin, M. J., and Rayner, N. A.: EN4: quality controlled ocean temperature and salinity profiles and monthly objective analyses with uncertainty estimates, *J. Geophys. Res. Oceans*, 118, 6704–6716, doi:10.1002/2013JC009067, 5 2013.
- Gouretski, V., and Reseghetti, F.: On depth and temperature biases in bathythermograph data: development of a new correction scheme based on analysis of a global ocean database, *Deep-Sea Res. PT. I*, 57, 6, doi:10.1016/j.dsr.2010.03.011, 2010.
- Hartung, K., Svensson, G., Struthers, H., Deppenmeier, A., and Hazeleger, W.: An EC-Earth coupled atmosphere-ocean single-column model (AOSCM) for studying coupled marine and polar process, *Geosci. Model Dev. Discuss.*, 10 doi:10.5194/gmd-2018-66, 2018.
- Hense, I., Stemmler, I., and Sonntag, S.: Ideas and perspectives: climate-relevant marine biologically driven mechanisms in Earth system models, *Biogeosciences*, 14, 403–413, doi:10.5194/bg-14-403-2017, 2017.
- Ichiye, T.: Some problem of circulation and hydrography of the Japan Sea and Tsushima Current. In: *Ocean Hydrography of the Japan Sea and China Seas*, edited by Ichiye, T., Elsevier Science Publishers, Amsterdam, 15–54, 1984. 15
- Jochum, M., Yeager, S., Lindsay, K., Moore K., and Murtugudde, R.: Quantification of the Feedback between Phytoplankton and ENSO in the Community Climate System Model, *J. Clim.*, 23, 2916–2925, doi:10.1175/2010JCLI3254.1, 2009.
- Joo, H. T., Park, J. W., Son, S. H., Noh, J.-H., Jeong, J.-Y., Kwak, J. H., Saux-Picart, S., Choi, J. H., Kang, C.-K., and Lee, S. H.: Long-term annual primary production in the Ulleung Basin as a biological hot spot in the East/Japan Sea, *J. Geophys. Res. Oceans*, 119, 3002–3011, doi:10.1002/2014JC009862, 2014. 20
- Kawabe, M. Branching of the Tsushima Current in the Japan Sea. Part II: Numerical experiment, *J. Oceanogr. Soc. Japan*, 38, 183–192, doi:10.1007/BF02111101, 1982.
- Kim, D.-W., Jo, Y.-H., Choi, J.-K., Choi, J.-G., and Bi, H.: Physical processes leading to the development of an anomalously large *Cochlodinium polykrikoides* bloom in the East sea/Japan sea, *Harmful Algae*, 55, 250–258, doi:10.1016/j.hal.2016.03.019, 2016. 25
- Kim, K., and Chung, J. Y.: On the Salinity-Minimum and Dissolved Oxygen-Maximum Layer in the East Sea (Sea Of Japan), *Elsev. Oceanogr. Serie.*, 39, 55–65, doi:10.1016/S0422-9894(08)70290-3, 1984.
- Kim, Y.-G., and Kim, K.: Intermediate Waters in the East/Japan Sea, *J. Oceanogr.*, 55, 123–132, doi:10.1023/A:1007877610531, 1999. 30
- Krezel, A., Szymanek, L., Kozłowski, L., and Szymelfenig, M.: Influence of coastal upwelling on chlorophyll a concentration in the surface water along the Polish coast of the Baltic Sea, *Oceanologia*, 47(4), 433–452, 2005.
- Large, W. G. and Yeager, S. G.: The global climatology of an interannually varying air-sea flux data set, *Clim. Dyn.*, 33, 341–364, doi:10.1007/s00382-008-0441-3, 2009.



- Lebassi-Habtezion, B., and Caldwell, P. M.: Aerosol specification in single-column Community Atmosphere Model version 5, *Geosci. Model Dev.*, 8, 817–828, doi:10.5194/gmd-8-817-2015, 2015.
- Lim, H.-G., Park, J.-Y., and Kug, J.-S.: Impact of chlorophyll bias on the tropical Pacific mean climate in an earth system model, *Clim. Dyn.*, doi:10.1007/s00382-017-4036-8, 2017.
- 5 Lips, I., and Lips, U.: Phytoplankton dynamics effected by the coastal upwelling events in the Gulf of Finland in July-August 2006, *J. Plankton Res.*, 32(9), 1269–1282, doi:10.1093/plankt/fbq049, 2010.
- Litchman, E., Pinto, P. T., Edwards, K. F., Klausmeier, C. A., Kremer, C. T., and Thomas M. K.: Global biogeochemical impacts of phytoplankton: a trait-based perspective, *J. Ecol.*, 103, 1384–1396, doi:10.1111/1365-2745.12438, 2015.
- Manizza, M., Le Quéré, C., Watson, A. J., and Buitenhuis, E. T.: Bio-optical feedbacks among phytoplankton, upper ocean  
10 physics and sea-ice in a global model, *Geophys. Res. Lett.*, 32, L05603, doi:10.1029/2004GL020778, 2005.
- McClain, C. R., Cleave, M. L., Feldman, G. C., Gregg, W. W., Hooker, S. B., and Kuring, N.: Science quality seawifs data for global biosphere research, *Sea Technol.*, 39, 10–16, 1998.
- Morel, A., and Antoine, D.: Heating rate within the upper ocean in relation to its Bio-Optical state, *J. Phys. Oceanogr.*, 24, 1652–1665, doi:10.1175/1520-0485(1994)024<1652:HRWTUO>2.0.CO;2, 1994.
- 15 Moriyasu, S.: The Tsushima Current. Kuroshio, Its Physical Aspects, 353–369 pp., 1972.
- Najjar, R., and Orr, J. C.: Design of OCMIP-2 simulations of chlorofluorocarbons, the solubility pump and common biogeochemistry, Internal OCMIP report, 25 pp., LSCE/CEA Saclay, Gif-sur-Yvette, France, 1998.
- National Institute of Fisheries Science, Korea Oceanographic Data Center, <http://www.nifs.go.kr/kodc>. (accessed May 20, 2018)
- 20 Park, J.-Y., Dunne, J. P., and Stock, C. A.: Ocean chlorophyll as a precursor of ENSO: An Earth system modeling study, *Geophys. Res. Lett.*, 45, 1939–1947, doi:10.1002/2017GL076077, 2018.
- Park, J.-Y., Kug, J.-S., Seo, H., and Bader, J.: Impact of bio-physical feedbacks on the tropical climate in coupled and uncoupled GCMs, *Clim. Dyn.*, 43, 1811–1827, doi:10.1007/s00382-013-2009-0, 2013.
- Price, J. F., Weller, R. A., and Pinkel, R.: Diurnal cycling: Observations and models of the upper ocean response to diurnal  
25 heating, cooling, and wind mixing, *J. Geophys. Res. Oceans*, 91, 8411–8427, doi:10.1029/JC091iC07p08411, 1986.
- Rho, T., Lee, T., Kim, G., Chang, K.-I., Na, T., and Kim, K.-R.: Prevailing Subsurface Chlorophyll Maximum (SCM) Layer in the East Sea and Its Relation to the Physico-Chemical Properties of Water Masses, *Ocean and Polar Res.*, 34(4), 413–430, doi:10.4217/OPR.2012.34.4.413, 2012. (in Korean)
- Sauerland, V., Löptien, U., Leonhard, C., Oschlies, A., and Srivastav, A.: Error assessment of biogeochemical models by  
30 lower bound methods (NOMMA-1.0), *Geosci. Model Dev.*, 11, 1181–1198, doi:10.5194/gmd-11-1181-2018, 2018.
- Shimomura, T. and Miyata K. The oceanographical conditions of the Japan sea and its water systems, laying stress on the summer of 1955, *Bull. Japan Sea Reg. Fish. Res. Lab.*, 6, 23–97, 1957. (in Japanese)



- Shin, J.-W., Park, J., Choi, J.-G., Jo, Y.-H., Kang, J. J., Joo, H. T., and Lee, S. H.: Variability of phytoplankton size structure in response to changes in coastal upwelling intensity in the southwestern East Sea, *J. Geophys. Res. Oceans*, 122, 10, 262–10, 274, doi:10.1002/2017JC013467, 2017.
- Sonntag, S., and Hense, I.: Phytoplankton behavior affects ocean mixed layer dynamics through biological-physical feedback mechanisms, *Geophys. Res. Lett.*, 38, L15610, doi:10.1029/2011GL048205, 2011.
- 5 Stock C. A., Dunne, J. P., and John, J. G.: Global-scale carbon and energy flows through the marine planktonic food web: an analysis with a coupled physical–biological model, *Progr. Oceanogr.*, 120, 1–28, doi:10.1016/j.pocean.2013.07.001, 2014.
- Tanioka, K.: On the Eastern Korea Warm Current (Tosen Warm Current), *Oceanogr. Mag.*, 20, 31–38, 1968.
- Uda, M.: The results of simultaneous oceanographical investigations in the Japan Sea and its adjacent waters in May and 10 June 1932, *J. Imp. Fisher. Exp. St.*, 5, 57–190, 1934. (in Japanese)
- Umlauf, L., and Burchard, H.: A generic length-scale equation for geophysical turbulence models, *J. Mar. Res.* 61, 235–265, doi:10.1357/002224003322005087, 2003.
- Umlauf, L., and Burchard, H.: Second-order turbulence closure models for geophysical boundary layers. A review of recent work, *Cont. Shelf Res.*, 25, 795–827, doi:10.1016/j.csr.2004.08.004, 2005.
- 15 Umlauf, L., Burchard, H., and Bolding, K.: General Ocean Turbulence Model. Scientific documentation. v3.2. Marine Science Reports no. 63, Baltic Sea Research Institute Warnemünde, 274 pp., Warnemünde, Germany, 2005.
- Wanninkhof, R.: Relationship between wind speed and gas exchange over the ocean, *J. Geophys. Res.*, 97, 7373–7382, doi:10.1029/92JC00188, 1992.
- Yool, A., Popova, E. E., and Anderson, T. R.: MEDUSA-2.0: an intermediate complexity biogeochemical model of the 20 marine carbon cycle for climate change and ocean acidification studies, *Geosci. Model Dev.*, 6, 1767–1811, doi:10.5194/gmd-6-1767-2013, 2013.

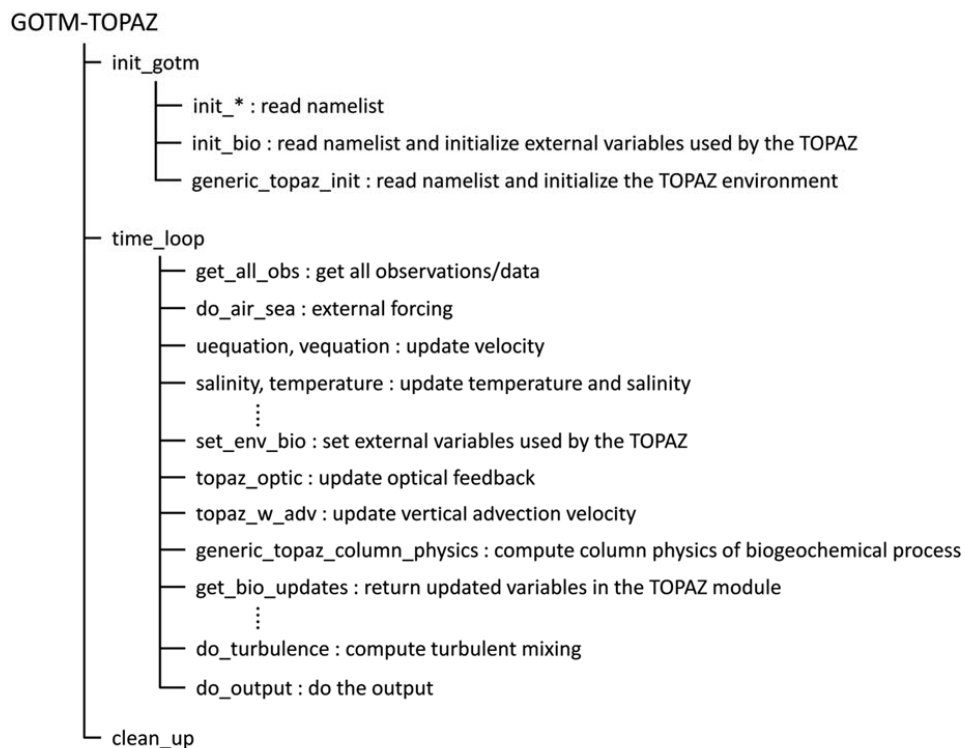
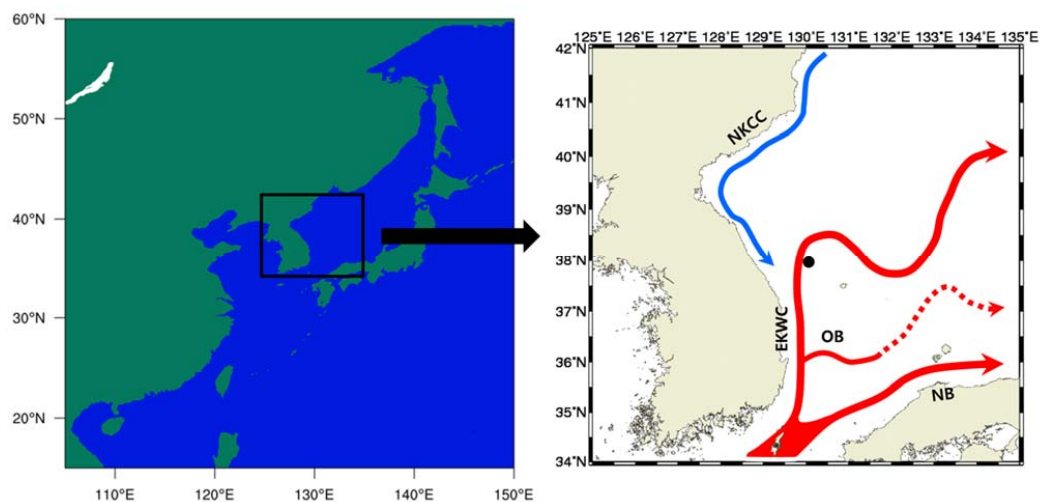


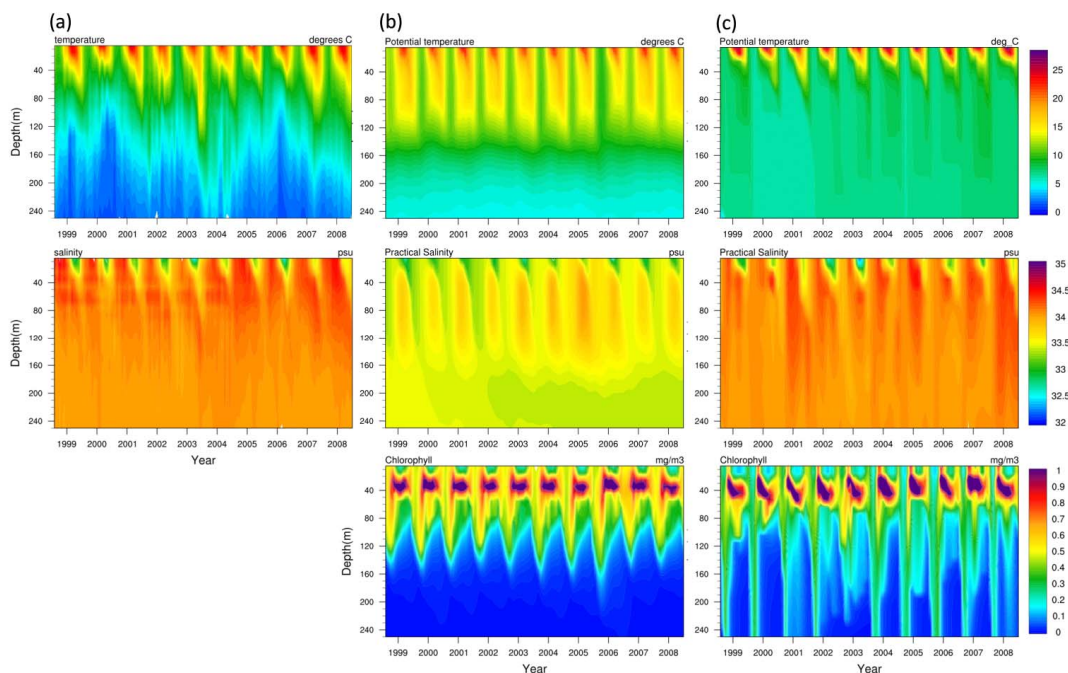
Figure 1: Flow diagram of the Fortran subroutines comprising GOTM-TOPAZ



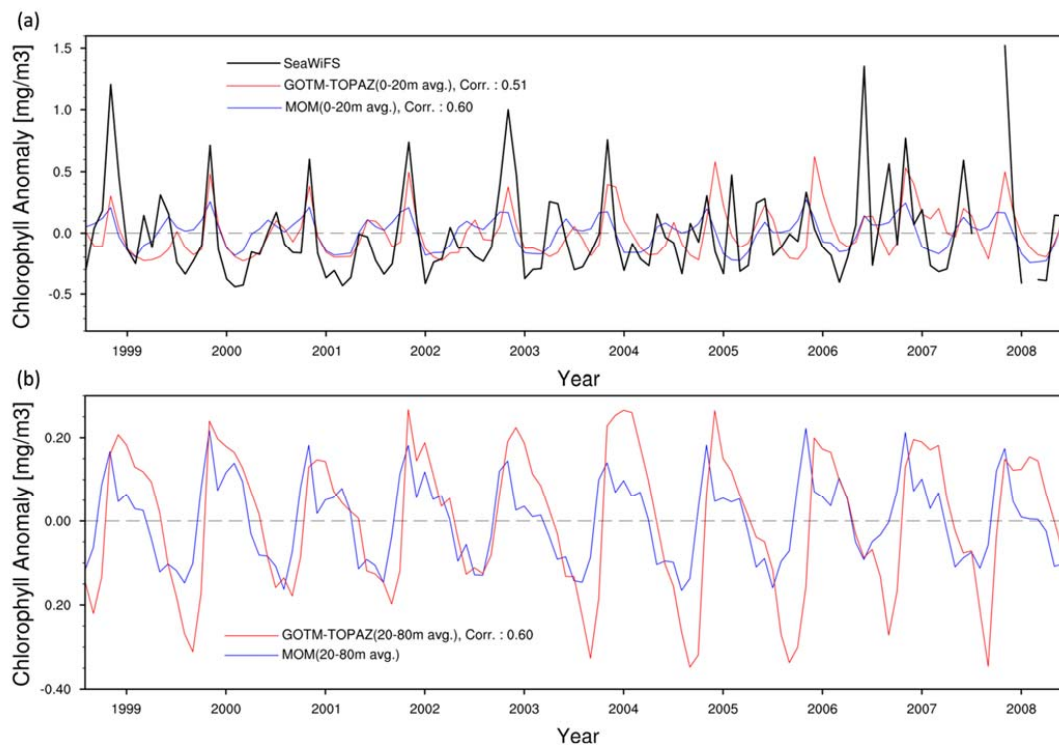
5

Figure 2: East/Japan Sea point (black point) and flow of the nearby North Korea Cold Current (NKCC), East Korea Warm Current (EKWC), Offshore Branch of the Tsushima Warm Current (OB), and the Nearshore Branch of the Tsushima Warm Current (NB)

10



5 **Figure 3: Comparison of the vertical spatial distribution over time for water temperature [°C], salinity [psu], and chlorophyll [mg m<sup>-3</sup>] for the period from 1999 to 2008; (a), (b), and (c) represent observational, MOM, and GOTM-TOPAZ results, respectively.**



5 **Figure 4: Chlorophyll anomaly time series and correlation values from observations (black line), MOM4p1\_SIS\_TOPAZ (blue line), and GOTM-TOPAZ (red line) for the period from 1999 to 2008; (a) chlorophyll anomaly of the two models representing the mean value for depths  $\geq 20$  m, along with the correlations between the observations and each model; (b) mean values at depths between 20 m and 80 m, along with the correlation between the two models.**

10

15

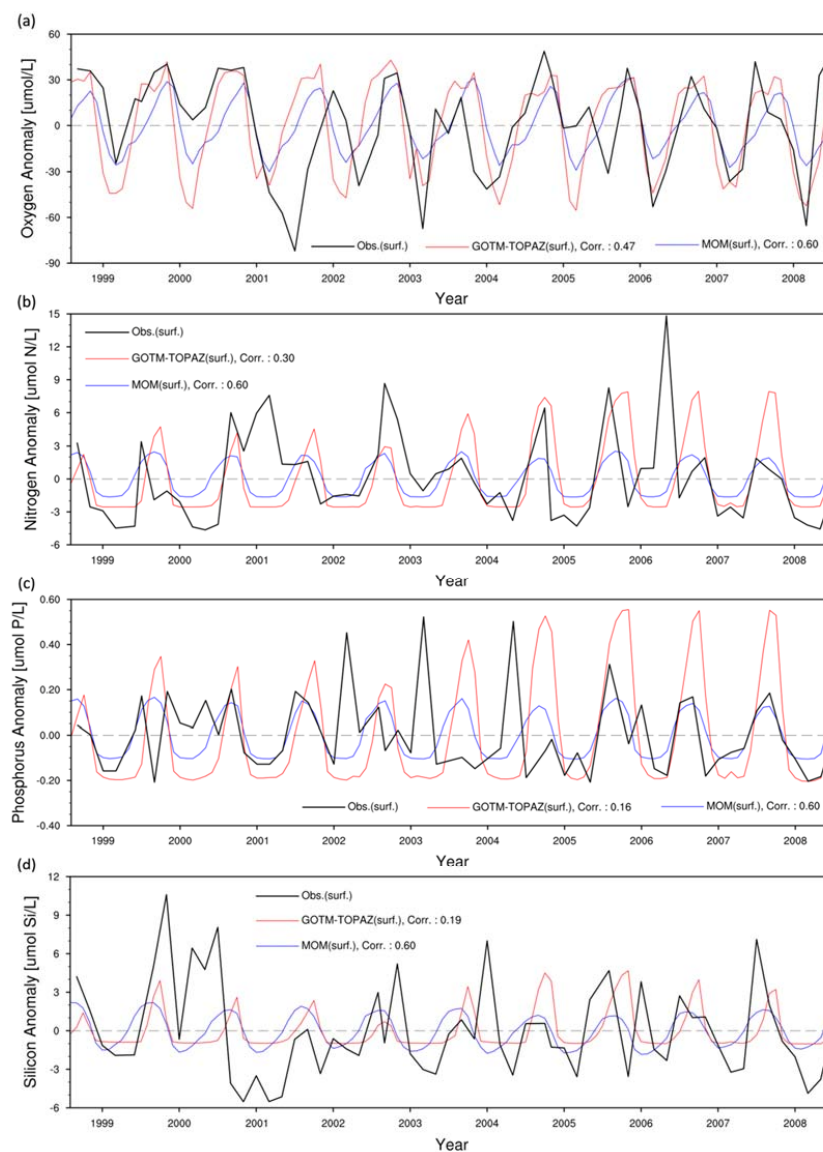


**Figure 5:** Anomaly time series and correlation values from observations (black line), MOM (blue line), and GOTM-TOPAZ (red line) with respect to (a) dissolved oxygen, (b) nitrogen, (c) phosphorus, and (d) silicon for the period from 1999 to 2008; in this figure, nitrogen, phosphorus, and silicon refers to the concentrations included in  $\text{NO}_3$ ,  $\text{PO}_4$ , and  $\text{SiO}_4$ , respectively.

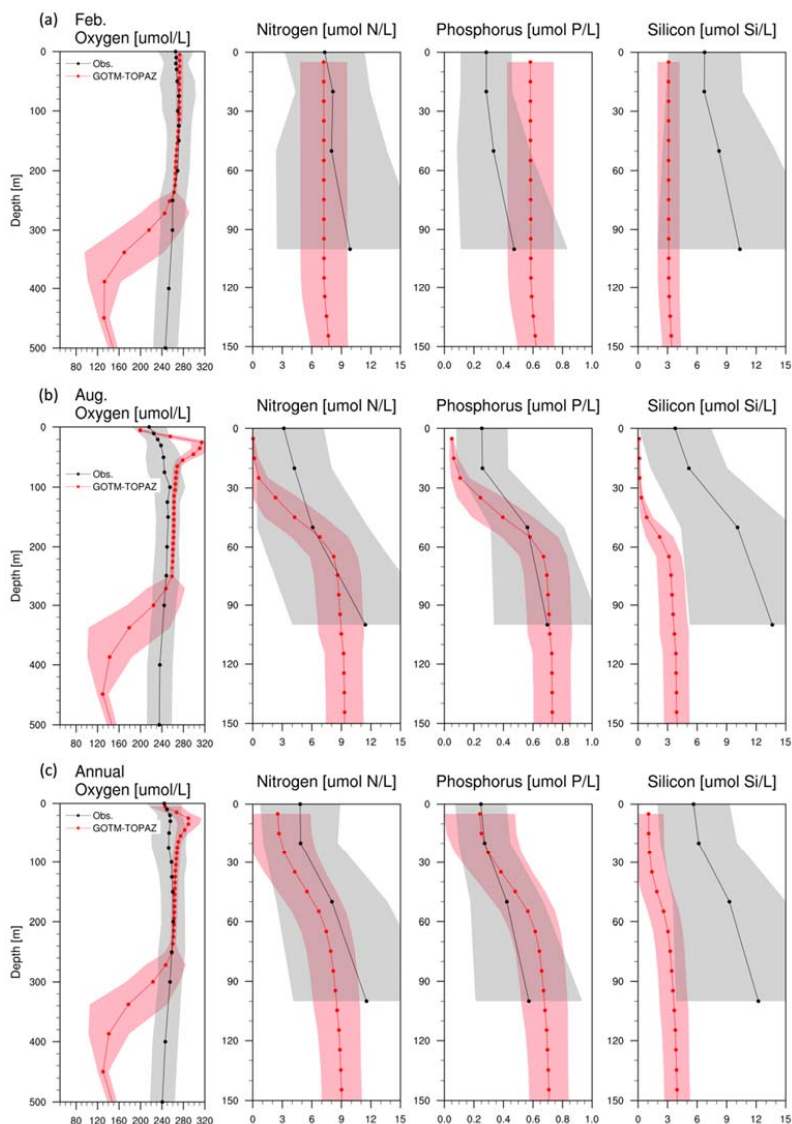


Figure 6: Vertical profile from the observations (black) and GOTM-TOPAZ (red) with respect to dissolved oxygen, nitrogen, phosphorus, and silicon averaged from 1999 to 2008; (a) average values for February; (b) average values for August; and (c) average annual values. Shaded area represents 1 sigma. In this figure, nitrogen, phosphorus, and silicon refers to the concentrations included in  $\text{NO}_3$ ,  $\text{PO}_4$ , and  $\text{SiO}_4$ , respectively.

5